Talanta 125 (2014) 439–445

Contents lists available at ScienceDirect

Talanta

journal homepage: www.elsevier.com/locate/talanta

Electrochemical immunosensor for detection of topoisomerase based on graphene–gold nanocomposites

Guang-Xian Zhong [a,b,1], Peng Wang [a,1], Fei-Huan Fu [d], Shao-Huang Weng [a], Wei Chen [a], Shao-Guang Li [a], Ai-Lin Liu [a,*], Zhao-Yang Wu [b], Xia Zhu [b], Xin-Hua Lin [a,*], Jian-Hua Lin [b,*], Xing-Hua Xia [c]

[a] Department of Pharmaceutical Analysis, Faculty of Pharmacy, Fujian Medical University, Fuzhou 350004, PR China
[b] Department of Orthopaedics, the First Affiliated Hospital of Fujian Medical University, Fuzhou 350004, PR China
[c] State Key Laboratory of Analytical Chemistry for Life Science, School of Chemistry and Chemical Engineering, Nanjing University, Nanjing 210093, PR China
[d] Department of Endocrinology, The County Hospital of Anxi, Anxi 362400, PR China

ARTICLE INFO

Article history:
Received 30 October 2013
Received in revised form
9 January 2014
Accepted 11 January 2014
Available online 16 February 2014

Keywords:
Electrochemical immunosensor
Graphene–gold nanocomposites
Topoisomerase

ABSTRACT

A facile electrochemical immunosensor based on graphene–three dimensional nanostructure gold nanocomposites (G–3D Au) using simple and rapid one-step electrochemical co-reduction technique was developed for sensitive detection of topoisomerase. The resultant G–3D Au nanocomposites were characterized by scanning electron microscopy, cyclic voltammetry and electrochemical impedance spectroscopy, and then were used as a substrate for construction of the "sandwich-type" immunosensor. Amperometric current–time curve was employed to monitor the immunoreaction on the protein modified electrode. The proposed method could respond to topoisomerase with a linear calibration range from 0.5 ng mL^{-1} to 50 ng mL^{-1} with a detection limit of 10 pg mL^{-1}. This new biosensor exhibited a fast amperometric response, high sensitivity and selectivity, and was successfully used in determining the topoisomerase which was added in human serum with a relative standard deviation ($n=5$) < 5%. The immunosensor served as a significant step toward the practical application of the immunosensor in clinical diagnosis and prognosis monitor.

1. Introduction

In recent years, electrochemical immunosensors have been of extensive interest in medical diagnosis and biological research due to their high sensitivity, small analyte volume, simple instrumentation, and minimal manipulation [1–6]. The introduction of nanomaterials and nanotechnologies has greatly improved the sensitivity and selectivity of electrochemical biosensors [7–13]. Recently, graphene–metal nanocomposites have attracted increasing attention due to their high electrocatalysis, biocompatibility and large active surface [14–16]. The graphene–metal nanocomposites are usually prepared by chemical or thermal reduction of mixtures of graphene (or graphite oxide) and metallic precursors [17–20]. However, in these methods, toxic reducing agents such as hydrazine hydrate or hydroquinone are introduced, thus extreme care should be made. Moreover, the chemical synthesis processes are time-consuming and require high temperature (95–100 °C) [21]. To overcome those drawbacks, the one-step electrochemical co-reduction of graphite oxide (GO) and metallic precursors has recently developed due to its simple, fast and green nature [22–24].

Topoisomerases are ubiquitous nuclear enzymes that regulate the overwinding or underwinding of DNA in eukaryotic cells. Several studies have demonstrated that topoisomerases could be used as prognostic markers for assessing the prognosis of different cancers such as osteosarcomas, breast ductal carcinomas and ovarian cancer, just to name a few examples [25–27]. Recently, many efforts have been made to develop various immunoassay methods including enzyme-linked immunosorbent assay (ELISA) [28], Western blot analysis [29] and immunohistochemistry [30] for detection of topoisomerases. However, these methods have some disadvantages such as tedious, time-consuming and expensive instruments. Therefore, it is necessary to develop a simple and sensitive method for quantitative detection of topoisomerases.

Herein, topoisomerase IIIβ was chosen as a detection topoisomerase model, and a highly sensitive electrochemical immunosensor based on graphene–three dimensional gold nanocomposites modified glassy carbon electrode (G–3D Au/GCE) was developed for detection of topoisomerase IIIβ (Scheme 1). The G–3D Au nanocomposites were

* Corresponding authors. Tel./fax: +86 591 22862016.
E-mail addresses: ailinliu@mail.fjmu.edu.cn (A.-L. Liu), xhl1963@sina.com (X.-H. Lin), jianhual@126.com (J.-H. Lin).
[1] Guang-Xian Zhong and Peng Wang contributed equally to the present study.

http://dx.doi.org/10.1016/j.talanta.2014.01.037
0039-9140

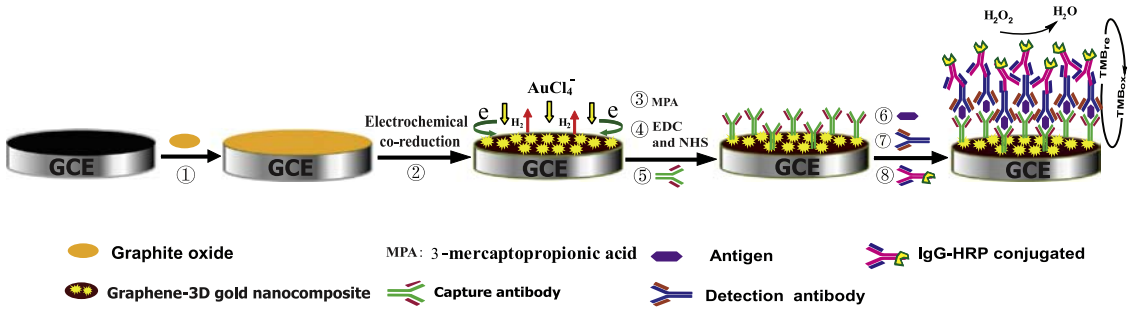

Scheme 1. Schematic representation of the fabrication procedure of the immunsensor based on graphene–3D nanostructure gold nanocomposite.

prepared by a one-step electrochemical co-reduction technique. The resultant G–3D Au/GCE was first covalently assembled with 3-mercaptopropionic acid (MPA) by Au–S bond, and then topoisomerase IIIβ primary antibodies (Ab1)/antigens/secondary antibodies (Ab2)/horseradish peroxidase (HRP) conjugated IgG were immobilized onto the electrode by immunoreaction to form an sandwich-type immunosensor. The electrochemical transduction was reached by the catalytic reduction of H_2O_2 by coupling with the redox reaction of 3,3′,5,5′-tetramethylbenzidine (TMB) at the electrode surface [31,32]. This method is cost-effective and versatile. The proposed immunosensing strategy allowed a rapid and sensitive means of topoisomerase IIIβ detection.

2. Materials and methods

2.1. Chemicals and materials

Mouse monoclonal anti-topoisomerase IIIβ (primary antibodies, Ab1, 100 ug) and rabbit purified polyclonal anti-topoisomerase IIIβ (secondary antibodies, Ab2, 50 ug) were purchased from Abnova Corporation (Taipei, Taiwan). The topoisomerase IIIβ recombinant protein (antigen, 10 ug) and the standard antigens solution (topoisomerase IIIβ 293T overexpression lysate) were obtained from Abnova Corporation (Taipei, Taiwan). The IgG-HRP conjugate was purchased from Abnova Corporation (Taipei, Taiwan). The antibody dilution was 10 mM phosphate-buffered saline (PBS buffer) containing 0.08 M NaCl (pH 7.4). The antibodies were aliquoted and stored at −20 °C. The purified antibodies were diluted upon usage in PBS suitable for the immobilizing and capture reactions. A commercial human topoisomerase IIIβ ELISA kit was purchased from CUSABIO (Wuhan, China), stored at 4 °C and used following the instructions given by the producers.

Natural powder graphite (sized ≤ 30 μm) was purchased from Shanghai Chemical Reagent Company. Tetrachloroaurate(III) tetrahydrate ($HAuCl_4 \cdot 4H_2O$, 47.8% Au), tris-(hydroxymethyl)aminomethane, 3-mercaptopropionic acid (MPA), nitric acid, sulfuric acid, potassium permanganate, ethanol, N-Hydroxysuccinimide (NHS), 1-Ethyl-3-(3-dimethylaminopropyl) carbodiimide hydrochloride (EDC) were provided by Sinopharm Chemical Reagent Co., Ltd. (China). Bovine serum albumin (BSA) was from Sigma-Aldrich (St. Louis, MO, USA). TMB substrate (Neogen K-blue low activity substrate) was purchased from Neogen (U.S.). All the chemicals were of analytical reagent grade and used without further purification. All solutions were prepared with Milli Q water (18 MΩ cm resistivity) from a Millipore system.

2.2. Apparatus

All electrochemical measurements were performed on a CHI 760D Electrochemical Workstation (CH Instrument, USA). Electrochemical experiments were carried out with a conventional three-electrode system comprising a platinum wire auxiliary electrode, an Ag/AgCl (with saturated KCl) reference electrode, and the modified glassy carbon electrode (GCE, diameter: 3 mm) as working electrode. Scanning electron microscopic (SEM) images were obtained from a Hitachi S-4800 scanning electron microscopy (Tokyo, Japan).

2.3. Preparation of G–3D Au/GCE

GO was synthesized from natural powder graphite by a modified Hummers' method [33,34]. Briefly, graphite powders were first oxidized by potassium permanganate in the presence of concentrated nitric acid and sulfuric acid for 30 min. After oxidation of graphite, the mixture was added to excess water, washed with a 5% HCl aqueous solution, and then repeatedly washed with water until the pH of filtrate reached neutral. The as-synthesized GO was suspended in water to give a brown dispersion, which was dialyzed for 1 week to completely remove residual salts and acids. Exfoliated graphite oxide (exfoliated GO) was obtained by ultrasound of the 1.0 mg mL^{-1} GO dispersion using a Sonifier. The obtained brown dispersion was then centrifuged at 3000 rpm for 5 min to remove any unexfoliated graphite oxide (an extremely small amount). The method to prepare G–3D Au/GCE was the same as that described in our previous report [35]. Briefly, GCE was polished successively with 1.0, 0.3 and 0.05 μm alumina powder to form a smooth, shiny surface. Then it was cleaned ultrasonically in 1:1 HNO_3, ethanol and Milli-Q water for 1 min, respectively, and dried with blowing N_2. An 8 μL exfoliated GO suspension was spread on a pretreated bare GCE using a micropipette tip. The film was dried in a vacuum desiccator. The GO-coated electrode was immersed in 2.8 mM $HAuCl_4$ and 0.1 M H_2SO_4 solution and a one-step electrochemical co-reduction was performed by cyclic voltammetry (CV) in a potential range from 0.0 to −1.5 V for a time of 900 s. The resultant G–3D Au/GCE was sonicated in deionized water and electrochemically cleaned by cycling the electrode potential between −0.35 and 1.5 V at 0.1 V s^{-1} in 0.5 M H_2SO_4 solution. The real surface of the clean electrode was calculated from the CV in 0.5 M H_2SO_4 solution.

2.4. Fabrication of the immunosensor

The cleaned G–3D Au/GCE was first dipped in 5 mM MPA aqueous solution for 24 h at room temperature. After thoroughly rinsed with deionized water to remove physically adsorbed MPA, it was immersed in a solution with 20 mg mL^{-1} of EDC and 10 mg mL^{-1} of NHS for 40 min. The activated MPA/G–3D Au/GCE was thoroughly rinsed with PBS, and then incubated overnight with 8 μl of Ab1 (0.1 mg mL^{-1}) to yield sensing interfaces. A blocking treatment aimed at preventing unspecific responses during the sample incubation was carried out by casting 15 μl of 5% (v/w) BSA at room temperature for 1 h, followed by washing carefully with PBS. Subsequently, 8 μl of the topoisomerase IIIβ antigen solution with different concentrations was added onto the

electrode surface and incubated for 1 h, and then the modified electrode was rinsed extensively to remove unbounded antigen molecules. After that, 8 μl of Ab_2 (0.02 mg mL^{-1}) was dropped onto the modified electrode surface and incubated for 1 h, followed by washing carefully with PBS. Finally, 8 μl of IgG-HRP conjugated (1:1000) was placed onto the electrode surface. After another 1 h, the electrode was washed and ready for measurement. The schematic illustration of the stepwise preparation of the immunosensor was shown in Scheme 1.

2.5. Electrochemical measurement

The electrochemical signal of the enzymatically produced TMB substrate was measured by CV and amperometric i–t curves. CV was carried out at a scan rate of 100 mV s^{-1}. Amperometric detection was performed at a fixed potential of 100 mV. Steady-state currents are recorded within 100 s. Electrochemical impedance measurements were carried out in a 0.1 M KCl solution containing 10 mM $K_3[Fe(CN)_6]$+10 mM $K_4[Fe(CN)_6]$ (1:1) by applying an alternating current voltage with 5 mV amplitude in a frequency range from 0.05 to 10^5 Hz. The data of condition, optimization, and calibration curve were the average of three measurements.

3. Results and discussion

3.1. Preparation of G–3D Au/GCE

A schematic representation of the immunosensor fabrication procedure was illustrated in Scheme 1. The G–3D Au/GCE was first prepared by a one-step electrochemical co-reduction method. The resultant G–3D Au/GCE was first covalently assembled with 3-mercaptopropionic acid (MPA) by Au–S bond, and then topoisomerase IIIβ primary antibodies (Ab1) were combined to the MPA-modified electrode by amide linkage to yield the sensing interface. After that, the unreacted covalent-active surface groups were passivated by bovine serum albumin (BSA). The topoisomerase IIIβ antigens, secondary antibodies (Ab2) and horseradish peroxidase (HRP) conjugated IgG were then immobilized onto the electrode by immunoreaction to form an IgG-HRP/Ab2/topoisomerase/Ab1/G–3D Au/GCE sandwich-type immunosensor. The HRP immobilized on the surface of electrode would offer an enzymatically amplified electrochemical current signal in TMB substrate. Notably HRP does not directly exchange electron with the electrode because its redox site is shielded within insulating peptide backbones. Therefore, small redox molecule TMB, as an electron shuttle, can diffuse in and out of the redox site of HRP.

Fig. 1A, B, and C were the SEM images of bare GCE, GO/GCE and G–3D Au/GCE, respectively. The SEM image of bare GCE showed a smooth morphology (Fig. 1A), while the SEM image of GO/GCE revealed the typically crumpled and wrinkled GO structure (Fig. 1B). Moreover, the SEM image of G–3D Au/GCE showed that pinecone-like 3D gold nanostructures and graphene sheets entangled with each other (Fig. 1C). The TEM images of GO/GCE and G–3D Au/GCE were shown in Fig. S1A and B. As shown in Fig. S1B, the gold nanoparticles in the scale of about 5–80 nm were deposited on the graphene sheets. The pinecone-like 3D gold nanostructures in Fig. 1C were composed of those gold nanoparticles. The formation mechanism of 3D gold nanostructure was as follows: firstly, the potential window in CV was set between 0.0 and −1.5 V to promote hydrogen bubble evolution. Then the hydrogen bubble evolved during the co-reduction process acted as a dynamic template for deposition of three-dimensional gold structures [36–38]. Fig. 1D was the energy-dispersive X-ray spectroscopy (EDS) spectrum of the G–3D Au nanocomposite. As shown in Fig. 1D, only C and Au peaks could be seen, indicating the successfully deposition of gold nanostructures on graphene sheets. The electroactive surface area of deposited 3D gold nanostructures could be evaluated from the coulombic integration of the reductive peak of gold oxide formed in the positive potential scan in 0.5 M H_2SO_4 [39]. To obtain the optimal co-reduction time, the influence of co-reduction time on electroactive surface area of Au was also investigated. As shown in Fig. 1E, the real active surface area was increased with the increasing co-reduction time and reached the maximum value at 900 s. Moreover, the maximum real active surface area was estimated to be 3.5 times larger than that of Au deposited on a GCE (Au/GCE) and 8.4 times larger than that of a planar Au electrode with the same geometric area (Fig. 1F) [39].

3.2. Electrochemical characteristics of the immunosensor based on G–3D Au/GCE

The preparation process of the electrochemical immunosensor was characterized by CV and electrochemical impedance spectroscopy (EIS). The CV behavior was performed in 10 mM $K_3Fe(CN)_6$ solution. As shown in Fig. 2A, it was clearly observed that the reversible redox peaks of $[Fe(CN)_6]^{3-}$ had a lowest peak current on the GO/GCE surface (inset, curve (c)), after electrochemical co-reduction of the GO with $HAuCl_4$, the reversible peaks increased greatly (inset, curve (a)), which was higher than the bare GCE (inset, curve (b)). The results indicated that the G–3D Au/GCE had accelerated electron transfer between the electrochemical probe $[Fe(CN)_6]^{3-}$ and the electrode. When the G–3D Au/GCE was functionalized with MPA (Fig. 2A, curve (b)), the reversible peaks decreased and the peak-to-peak separation increased compared with the bare G–3D Au/GCE (Fig. 2A, curve (a)), suggesting that the electron transfer between the electrochemical probe and electrode surface was inhibited, owing to the electrostatic repulsion of Fe$(CN)_6^{3-}$ anion and the negatively charged MPA. After immobilization of Ab1 and BSA, the peak currents of Fe$(CN)_6^{3-}$ decreased significantly due to the blockage of biomacromolecules on the electrode surface (curves (c and d)). When the topoisomerase IIIβ antigen, Ab2 and IgG-HRP molecules were combined to the electrode surface by immunoreaction, the peak currents of Fe$(CN)_6^{3-}$ decreased again (curves (e, f, and g)), owing to the blockage of biomacromolecules on the electrode surface.

In order to further evaluate the preparation process of the electrochemical immunosensor, EIS was performed in a solution of 0.1 M KCl containing 10 mM $[Fe(CN)_6]^{3-/4-}$. The impedance spectra include a semicircle portion and a linear portion. The semicircle portion at higher frequencies corresponds to the electron-transfer limited process, and the linear portion at lower frequencies represents the diffusion-limited process. The charge transfer resistance R_{et} can be directly measured as the semicircle diameter. Fig. 2B showed the impedance spectra observed upon the stepwise modification process. As shown in Fig. 2B, when the electrode was conjugated with MPA, the R_{et} was slightly increased (curve b) compared with bare G–3D Au/GCE (curve a), showing that the self-assembled layers of COO^- terminal groups on the electrode surface generated a negatively charged surface that reduced the ability of the redox probe to access the layer. When the Ab1 molecules were attached to the G–3D Au/GCE, R_{et} increased (curve c), and R_{et} increased again after the electrode was blocked with BSA (curve d). This phenomenon could be explained in which the protein layer on the electrode surface acted as barrier to the interfacial electron transfer, leading to an increase in R_{et}. In particular, when the prepared immunosensor was incubated with topoisomerase IIIβ antigen solution, the formed antigen–antibody immonocomplex on the film would further hinder the access of the redox probe to the electrode (curves e). Furthermore, R_{et} increased in the same way when the Ab2 and IgG-HRP molecules

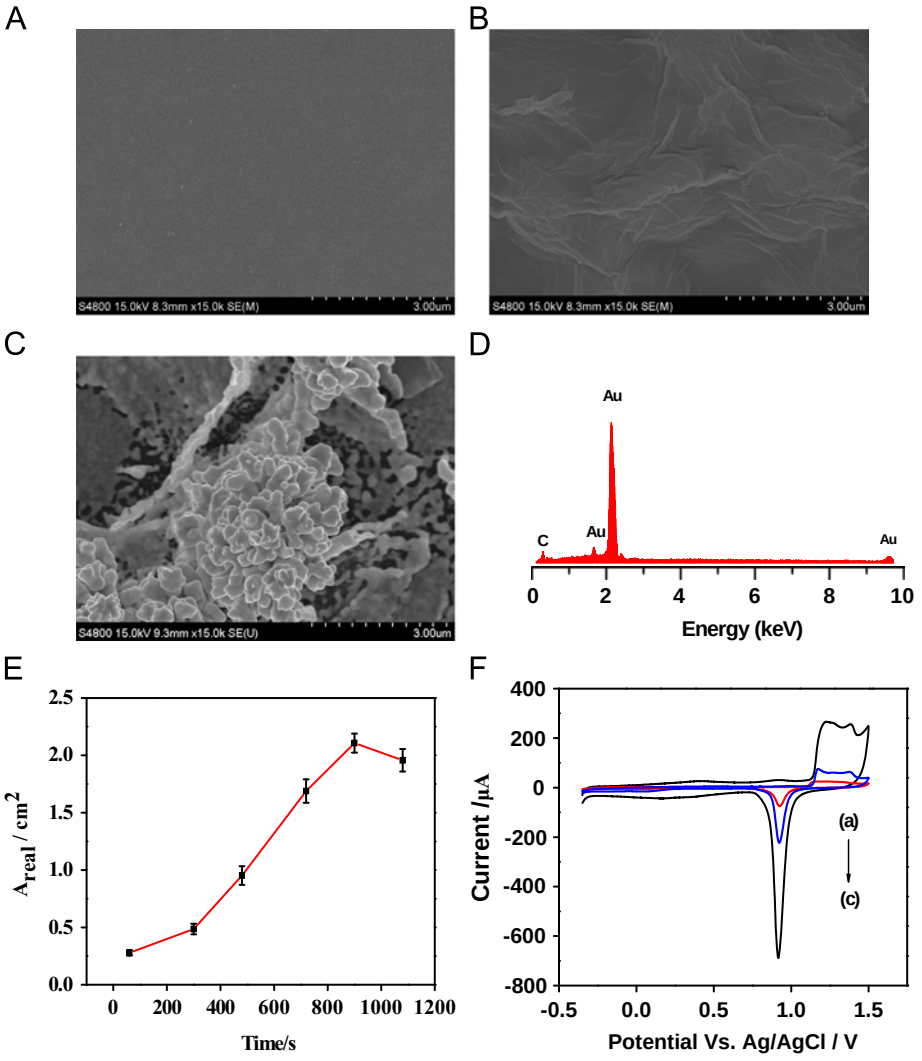

Fig. 1. (A) SEM images of bare GCE, (B) GO/GCE, and (C) G–3D Au/GCE. (D) EDS spectrum of G–3D Au on the GCE. (E) Effect of the co-reduction time on real surface area of god deposited at G–3D Au/GCE by integration of the reduction peak of CVs in a solution of 0.5 M H_2SO_4 at a scan rate of 100 mV/s. (F) Cyclic voltammograms (CVs) of a G–3D Au/GCE (curve (c)), Au/GCE (curve (b)) and a planar gold electrode (curve (a)) with the same geometric area in a solution of 0.5 M H_2SO_4 at a scan rate of 100 mV/s.

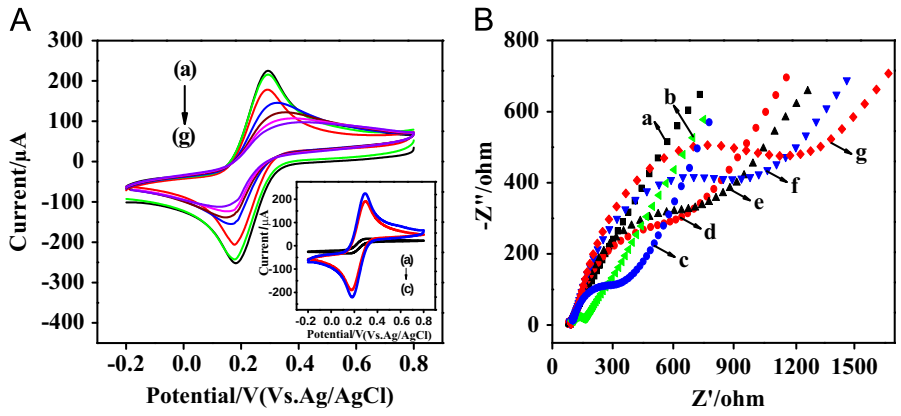

Fig. 2. (A) Cyclic voltammograms (CVs) of different modified electrodes in 10 mM $[Fe(CN)_6]^{3-}$ and 0.1 M KCl solution at scan rate of 100 mV/s, (a) bare G–3D Au/GCE, (b) MPA/G–3D Au/GCE, (c) Ab1/MPA/G–3D Au/GCE, (d) BSA/Ab1/MPA/G–3D Au/GCE, (e) Antigen/Ab1/MPA/G–3D Au/GCE, (f) Ab2/Antigen/Ab1/MPA/G–3D Au/GCE, (g) HRP-IgG/Ab2/Antigen/Ab1/MPA/G–3D Au/GCE. Inset was the CVs of (a) bare G–3D Au/GCE, (b) bare GCE, and (c) bare GO/GCE. (B) Impedance spectras (Nyquist plots) of (a) bare G–3D Au/GCE, (b) MPA/G–3D Au/GCE, (c) Ab1/MPA/G–3D Au/GCE, (d) BSA/Ab1/MPA/G–3D Au/GCE, (e) Antigen/Ab1/MPA/G–3D Au/GCE, (f) Ab2/Antigen/Ab1/MPA/G–3D Au/GCE and (g) HRP-IgG/Ab2/Antigen/Ab1/MPA/G–3D Au/GCE. The data are recorded in the presence of 10 mM $[Fe(CN)_6]^{4-/3-}$ as redox label. The biased potential is 0.21 V (versus Ag/AgCl) in the frequency range from 0.05 to 10^5 Hz and the amplitude is 5.0 mV.

were combined to the electrode surface by immunoreaction (curves f and g). The EIS change of the modified process was in good agreement with the CV results, indicated that the IgG-HRP/Ab2/topoisomerase IIIβ/Ab1/G–3D Au composite film was successfully formed on electrode surface and suitable for immunosensing. Moreover, due to the good conductivity of the G–3D Au nanocomposite demonstrated by

our previous study [35], the value of R_{et} at G–3D Au/GCE was lower than that of at planar gold electrode [40].

3.3. The electrochemical response of the immunosensor based on G–3D Au/GCE

The i–t curves of capture antibody or capture antibody/antigen/detection antibody sandwich modified biosensor at different electrodes in TMB solution was showed in Fig. S2. As shown in Fig. S2, after immunoreaction with antigen and detection antibody (curves c and d), the amperometric current intensity increased significantly. This could be explained that upon immunoreaction, the HRP was bound onto the surface of electrode by the formation of sandwich structure, and the HRP could efficiently catalyze reduction reactions of H_2O_2 with the redox reaction of TMB, leading to significant amplification of reduction current [31,32]. However, due to the absence of the antibody conjugated with HRP, this catalytic reduction current on the capture antibody modified biosensor was not obvious. The difference in reduction peak current at G–3D Au/GCE in Fig. S2 (curves b and d) was about 4.1 times as large as that at planar gold electrode in Fig. S2 (curves a and c), demonstrating that the G–3D Au/GCE-based biosensor could immobilized antibody more efficiently.

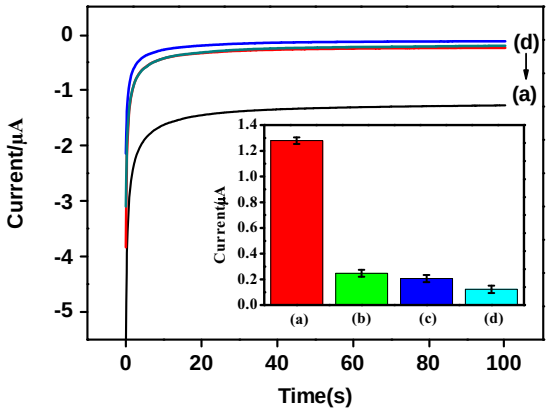

Fig. 3. Amperometric response of the immunosensor to different antigens with the same concentration. (a) topoisomerase IIIβ antigen, (b) AFP-antigen, (c) CEA-antigen and (d) Blank solution.

3.4. The specificity of the immunosensor

Specificity is an important parameter which influences the performance of an immunosensor in practical application. In order to confirm that the presented sensor responds only to topoisomerase IIIβ antigen but not to the nonspecific adsorption of other proteins, contrast experiments were performed. After immobilization of topoisomerase IIIβ antibody and blocking with BSA, the electrodes were exposed to topoisomerase IIIβ antigen, AFP-antigen and CEA-antigen with the same concentration of 10 ng mL^{-1}. Fig. 3 showed the i–t curves that correspond to current intensity arised from the immunoreaction of topoisomerase IIIβ antibody with different proteins. As shown in Fig. 3, the amperometric current intensity increased greatly after immunoreaction with topoisomerase IIIβ antigen as compared with blank solution. No remarkable change of current was observed when the topoisomerase IIIβ antibody reacted with AFP-antigen and CEA-antigen. This phenomenon indicated that the observed current changes were due to specific antibody–antigen interaction, and the presence of other proteins seemed not to interfere with the sensor performance. Thus, the proposed immunosensor showed good selectivity.

3.5. Performance of the immunosensor

To further evaluate the detection performance of the G–3D Au nanocomposite-based biosensor, the amperometric signals were measured before and after immunoreaction with the topoisomerase IIIβ antigen at different concentrations. As shown in Fig. 4A, the current increased with the increase of the concentration of topoisomerase IIIβ antigen in the range from 0.05 ng mL^{-1} to 100 ng mL^{-1} (shown in Fig. 4, inset). A good linear relationship between the current signal and the logarithmic value of antigen concentrations was observed (shown in Fig. 4B) in a range from 0.5 ng mL^{-1} to 50 ng mL^{-1}. The linear regression equation was $I\,(\mu A) = 0.4702 + 0.4809 \lg C_{Topo\ III\beta}\ (ng\ mL^{-1})$, $R = 0.9956$. A detection limit of 10 pg mL^{-1} TopoIIIβ antigen could be estimated using 3σ (where σ is the standard deviation of the blank solution, $n = 5$). The reproducibility of the biosensor for detection of 10 ng mL^{-1} topoisomerase IIIβ antigen was 7.46% ($n = 5$). According to the linear equation, the concentration of topoisomerase IIIβ antigen could be detected by an appropriate dilution with pH 7.4 PBS. As shown in Table 1, the detection limit of the present immunosensor was similar with those immunosensors modified with other nanocomposites [41–44], but the preparation process of G–3D Au was more simple and green than those nanocomposites.

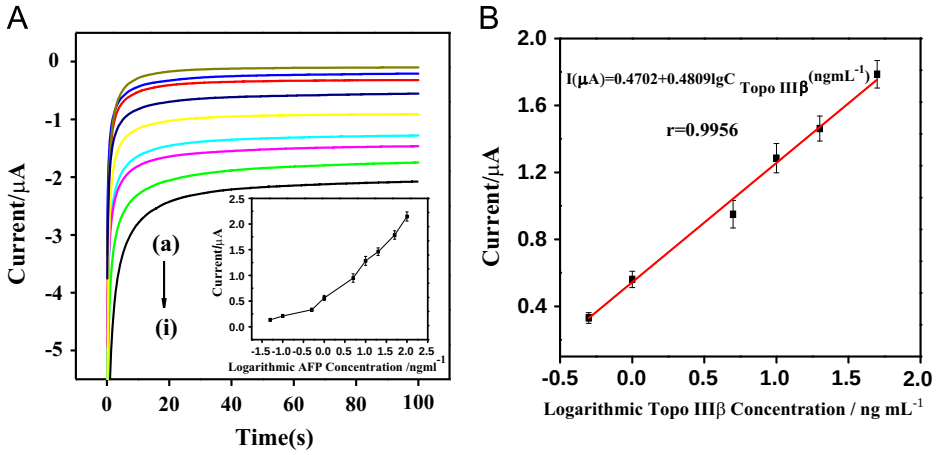

Fig. 4. (A) Current–time curves that corresponded to the G–3D Au/GCE before and after incubating with different concentrations of topoisomerase IIIβ antigen in TMB solution. (a) blank solution; curves (b–i) represent 0.05, 0.5, 1.0, 5.0, 10.0, 20.0, 50.0, 100.0 ng mL^{-1} topoisomerase IIIβ antigen, respectively. Inset shows calibration curve of currents versus logarithmic topoisomerase IIIβ antigen concentration, where the definition of signal is the same as that in Fig. 4A. (B) The linear relationship between currents and logarithmic topoisomerase IIIβ antigen concentration (from 0.5 ng mL^{-1} to 50 ng mL^{-1}).

Table 1
Comparison of different electrochemical immunosensors.

Material of the modified electrode	Linear range (ng mL^{-1})	Detection limit (ng mL^{-1})	References
Gold nanoparticles and carbon nano-tubes doped chitosan (GNP/CNT/Ch)	1.0–55.0	0.6	[36]
Nanogold/toluidine blue/poly-sulfanilic acid (nanogold/TB/PSAA)	0.5–120	0.2	[37]
Au nanoparticles/muli-wall carbon nanotubes-chitosans (AuNPs/MWCNTs-Chits)	0.3–20	0.01	[38]
Gold nanoparticle/reduced graphene oxide/poly (L-arginine) (AuNPs/R-GO/Arg)	0.5–200	0.03	[39]
Graphene–three dimensional nanostructure gold nanocomposites (G–3D Au)	0.5–50	0.01	This work

Table 2
Comparison of the developed immunosensor and ELISA kit in detection the concentration of topoisomerase IIIβ 293T overexpression lysate ($n=5$).

Sample (ng mL^{-1})	Developed immunosensor (ng mL^{-1})	R.S.D. (%)	Recovery (%)	ELISA (ng mL^{-1})
20	20.5	2.9	102.5	19.8
5	4.7	3.8	94	5.1
1	1.1	4.5	110	0.9

3.6. Precision, reproducibility, and stability of the developed immunosensor

To evaluate the reproducibility of the immunosensor, a series of three electrodes was prepared for the detection of 10.0 ng mL^{-1} topoisomerase IIIβ antigen. The relative standard deviation (RSD) of the measurements for three electrodes was 4.72%, indicating acceptable precision and fabrication reproducibility. The immunosensor could retain its current response after a storage period of 30 days in PBS (10 mM, pH 7.4) at 4 °C, without obvious decline, showing good stability of the developed immunosensor. According to the reported method [45], the regeneration of the immunosensor was developed by rinsing with stripping buffer of 0.1 M glycine-HCl (pH 2.2) for 3 min to dissociate the Ag–Ab complex. The as-renewed immunosensor could restore 95% of the initial value after 5 times regeneration, showing high reusability and stability.

3.7. Real sample analysis

The applicability of new electrochemical immunosensor to real samples was demonstrated by analyzing an artificial serum sample. The artificial serum sample was made up by directly adding an amount of topoisomerase IIIβ 293T overexpression lysate to a normal person serum sample. The concentration of topoisomerase IIIβ in the artificial serum sample was then determined with proposed immunosensor and ELISA. From the results shown in Table 2, it was clearly observed that the developed immunosensor had strong resistibility to the complex matrix of serum sample and could be used to directly detect quantitative topoisomerase IIIβ in real serum samples, and the results obtained using the developed immunosensor were in good agreement with the results obtained from ELISA. The R.S.D. less than 5% in 5 experiments were in the acceptable range. Thus, this method has potential application in detection of the topoisomerase IIIβ levels in the clinical real samples.

4. Conclusion

In this work, we have designed a new sandwich-type electrochemical immunosensor based on G–3D Au/GCE for the sensitive detection of topoisomerase. The G–3D Au nanocomposites, which were synthesized by facile and rapid one-step electrochemical co-reduction technique, could enhanced the conductivity and enlarge the specific surface area of the sensing interface. Thus, the G–3D Au nanocomposites would be useful for immobilizing antibody more efficiently. Furthermore, the enhanced sensitivity of the developed immunosensor was also achieved by introducing the bioconjugates of IgG-HRP onto the electrode surface through "sandwich" immunoreactions. The present topoisomerase immunosensor exhibited attractive features such as fast response, high selectivity and sensitivity, good accuracy. The proposed method can be observed to improve the immunoassay performance, and should have wide applications in the diagnosis and prognosis monitoring of cancers or other immunoassay.

Acknowledgments

The authors gratefully acknowledge the financial support of the National High Technology and Development of China (2012AA022604), the National Natural Science Foundation of China (20975021, 21275028, and 81301520), Sponsored by Medical Elite Cultivation Program of Fujian, P.R.C (2013-ZQN-JC-5), the science and technology plan project of General Administration of Quality Supervision (2014IK060), and the Scientific Research Major Program of Fujian Medical University (09ZD013), Research Fund for the Doctoral Program of Higher Education of China (20123518110001), the Fujian Provincial Important Science and technology Foundation (2011R1007-2), Foundation of Fujian Provincial Department of Education (JA11110 and JA12130), and The key Clinical Specialty Discipline Construction Program of Fujian, P.R. China.

Appendix A. Supporting information

Supplementary data associated with this article can be found in the online version at http://dx.doi.org/10.1016/j.talanta.2014.01.037.

References

[1] B.J. Privett, J.H. Shin, M.H. Schoenfisch, Anal. Chem. 80 (2008) 4499.
[2] G.F. Wang, X. Gang, X. Zhou, G. Zhang, H. Huang, X.J. Zhang, L. Wang, Talanta 103 (2013) 75.
[3] H.F. Chen, D.P. Tang, B. Zhang, B.Q. Liu, Y.L. Cui, G.N. Chen, Talanta 91 (2012) 95.
[4] S.K. Mishra, D. Kumar, A.M. Biradar, Rajesh, Bioelectrochemistry 88 (2012) 118.
[5] G.K. Parshetti, F.H. Lin, R.A. Doong, Sens. Actuators B: Chem. 186 (2013) 34.
[6] J.X. Li, G. Liu, W. Zhang, W. Cheng, H.B. Xu, S.J. Ding, J. Electroanal. Chem. 708 (2013) 95.
[7] D.P. Tang, R. Yuan, Y.Q. Chai, Anal. Chem. 80 (2008) 1582.
[8] J. Tang, R. Hu, Z.S. Wu, G.L. Shen, R.Q. Yu, Talanta 85 (2011) 117.
[9] Y.J. Lai, J. Bai, X.H. Shi, Y.B. Zeng, Y.Z. Xian, J. Hou, L.T. Jin, Talanta 107 (2013) 176.
[10] J.J. Lu, S.Q. Liu, S.G. Ge, M. Yan, J.H. Yu, X.T. Hu, Biosens. Bioelectron. 33 (2012) 29.
[11] K.J. Huang, D.J. Niu, J.Y. Sun, J.J. Zhu, J. Electroanal. Chem. 656 (2011) 72.
[12] K.J. Huang, J. Li, Y.Y. Wu, Y.M. Liu, Bioelectrochemistry 90 (2013) 18.
[13] H.P. Peng, Y. Hu, A.L. Liu, W. Chen, X.H. Lin, X.B. Yu, J. Electroanal. Chem. 712 (2014) 89.
[14] Y. Liu, H.B. Feng, Y.M. Wu, L. Joshi, X.Q. Zeng, J.H. Li, Biosens. Bioelectron. 35 (2012) 63.
[15] B.L. Su, J. Tang, J.X. Huang, H.H. Yang, B. Qiu, G.N. Chen, D.P. Tang, Electroanalysis 22 (2012) 2720.
[16] S. Yu, X.Y. Cao, M Yu, Microchem. J. 103 (2012) 125.
[17] C. Xu, X. Wang, J.W. Zhu, J. Phys. Chem. C 112 (2008) 19841.
[18] Y.C. Si, E.T. Samulski, Chem. Mater. 20 (2008) 6792.
[19] R. Pasricha, S. Gupta, A.K. Srivastava, Small 5 (2009) 2253.

[20] E. Yoo, T. Okata, T. Akita, M. Kohyama, J. Nakamura, I. Honma, Nano Lett. 9 (2009) 2255.
[21] Z.J. Wang, X.Z. Zhou, J. Zhang, F. Boey, H. Zhang, J. Phys. Chem. C 113 (2009) 14071.
[22] Y.G. Zhou, J.J. Chen, F.B. Wang, Z.H. Sheng, X.H. Xia, Chem. Commun. 46 (2010) 5951.
[23] C.P. Fu, Y.F. Kuang, Z.Y. Huang, X. Wang, N.N. Du, J.H. Chen, H.H. Zhou, Chem. Phys. Lett. 499 (2010) 250.
[24] C.B. Liu, K. Wang, S.L. Luo, Y.H. Tang, L.Y. Chen, Small 7 (2011) 1203.
[25] N. Entz-Werle, E. Guerin, P. Marec-Berard, M. Tabone, C. Schmitt, J. Gentet, H. Pacquement, L. Brugieres, C. Kalifa, A. Babin, M. Gaub, J. Clin. Oncol. 26 (2008) 10030.
[26] J.P. Oliveira-Costa, J. Zanetti, L.R. Oliveira, F.A. Soares, L.Z. Ramalho, F. Silva Ramalho, S.B. Garcia, A. Ribeiro-Silva, Hum. Pathol. 41 (2010) 1624.
[27] W.H. Gotlieb, I. Goldberg, B. Weisz, B. Davidson, I. Novikov, J. Kopolovic, G. Ben-Baruch, Gynecol Oncol. 82 (2001) 99.
[28] S. Sato, Y. Hamaguchi, M. Hasegawa, K. Takehara, Rheumatology (Oxford) 40 (2001) 1135.
[29] L. Liebes, M. Potmesil, T. Kim, D. Pease, M. Buckley, D. Fry, J. Cho, H. Adler, K. Dar, A. Zeleniuch-Jacquotte, H. Hochster, Clin. Cancer Res. 4 (1998) 545.
[30] H. Hafian, L. Venteo, A. Sukhanova, I. Nabiev, B. Lefevre, M. Pluot, Hum. Pathol. 35 (2004) 745.
[31] G. Liu, Y. Wan, V. Gau, J. Zhang, L. Wang, S. Song, C. Fan, J. Am. Chem. Soc. 130 (2008) 6820.
[32] P. Fanjul-Bolado, M.B. Gonzalez-Garcia, A. Costa-Garcia, Anal. Bioanal. Chem. 382 (2005) 297.
[33] N.I. Kovtyukhova, P.J. Ollivier, B.R. Martin, T.E. Mallouk, S.A. Chizhik, E.V. Buzaneva, A.D. Gorchinskiy, Chem. Mater. 11 (1999) 771.
[34] W.S. Hummers, R.E. Offeman, J. Am. Chem. Soc. 80 (1958) 1339.
[35] A.L. Liu, G.X. Zhong, J.Y. Chen, S.H. Weng, H.N. Huang, W. Chen, L.Q. Lin, Y. Lei, F.H. Fu, Z.L. Sun, X.H. Lin, J.H. Lin, S.Y. Yang, Anal. Chim. Acta 767 (2013) 50.
[36] F. Li, X.P. Han, S.F. Liu, Biosens. Bioelectron. 26 (2011) 2619.
[37] Y. Li, Y.Y. Song, C. Yang, X.H. Xia, Electrochem. Commun. 9 (2007) 981.
[38] S. Yang, W.Z. Jia, Q.Y. Qian, Y.G. Zhou, X.H. Xia, Anal. Chem. 81 (2009) 3478.
[39] S. Trasatti, O.A. Petrii, J. Electroanal. Chem. 327 (1992) 353.
[40] J.Y. Park, Y.S. Lee, B.H. Kim, S.M. Park, Anal. Chem. 80 (2008) 4986.
[41] J. Lin, C. He, L. Zhang, S. Zhang, Anal. Biochem. 384 (2009) 130.
[42] X. Li, R. Yuan, Y. Chai, L. Zhang, Y. Zhuo, Y. Zhang, J. Biotechnol. 123 (2006) 356.
[43] K.J. Huang, D.J. Niu, W.Z. Xie, W. Wang, Anal. Chim. Acta 569 (2010) 102.
[44] S. Yu, X.Y. Cao, M. Yu, Microchem. J. 103 (2012) 125.
[45] J.H. Lin, Z.J. Wei, H.H. Zhang, M.J. Shao, Biosens. Bioelectron. 41 (2013) 342.